PERGAMON

International Journal of Multiphase Flow 28 (2002) 707–729

International Journal of Multiphase Flow

www.elsevier.com/locate/ijmulflow

Prediction of the transition from stratified to slug and plug flow for long pipes

E.T. Hurlburt, T.J. Hanratty *

Department of Chemical Engineering, University of Illinois, 600 South Mathews Avenue, Urbana, IL 61801, USA

Received 1 March 2000; received in revised form 29 December 2001

Abstract

Theoretical relations that can be used to predict transition from a stratified pattern to an intermittent pattern for gas–liquid flow in long pipes are presented. These include Kelvin–Helmholtz theory, viscous long wavelength theory, the necessary conditions for a slug to be stable (slug stability theory), and the definition of a plug flow. Comparisons are made with measurements of transition taken in systems over a range of pipe diameters and a range of fluid properties. An important result is that slug stability defines transition in flows with high gas density. A methodology for predicting transition is proposed. © 2002 Elsevier Science Ltd. All rights reserved.

Keywords: Gas–liquid pipe flow; Flow regime transition; Slug flow; Plug flow; Stability of slugs

1. Introduction

The concurrent passage of gas and liquid in a horizontal pipe results in a variety of patterns. For relatively low gas and liquid rates a stratified configuration occurs with the liquid flowing on the bottom and the gas flowing above it. As the liquid rate is increased (at a constant gas rate) waves appear on the interface. At still higher liquid rates the waves can grow to the top of the pipe and, intermittently, form liquid blockages. At low gas velocities this intermittent regime is characterized as a plug pattern, whereby the gas flows as steady elongated bubbles along the top of the pipe. At high gas flows a slug pattern exists whereby slugs of highly aerated liquid move downstream approximately at the gas velocity. The fronts of the liquid slugs are unsteady hydraulic jumps.

* Corresponding author. Tel.: +1-217-333-1318; fax: +1-217-333-5052.
E-mail address: thanratt@uiuc.edu (T.J. Hanratty).

PII: S0301-9322(02)00009-5

The main theoretical approach to predicting the transition to slug or plug flow in a long pipe has been to consider the stability of a stratified pattern. This examination needs to be accompanied by experimental observation because the outcome of the instability is not predicted. A simplification is to use a linear analysis. The assumption of an inviscid gas–liquid flow and a long wavelength disturbance yields the following critical condition for flow in a two-dimensional channel with a height, $h = h_G + h_L$:

$$\rho_G\left(\overline{U} - \bar{u}\right)^2 = \rho_L g \epsilon h \tag{1}$$

where $\overline{U}$ is the velocity of the gas, $\bar{u}$, the velocity of the liquid, g, the acceleration due to gravity, ϵ, the volume fraction of the gas. The velocity of the unstable waves is given as

$$C \cong \bar{u} \tag{2}$$

for small ρ_G/ρ_L. Eq. (1) predicts that a critical gas velocity is reached when the destabilizing effect of wave-induced pressure variations in the gas overcome the restoring force of gravity.

Wallis and Dobbins (1973) found that Eq. (1) overpredicts the critical gas velocity by a factor of about 2. Taitel and Dukler (1976) argued that non-linear effects need to be taken into account and suggested the following critical conditions for flow in a channel and for flow in a pipe with diameter D:

$$\rho_G\left(\overline{U} - \bar{u}\right)^2 = \left(1 - \frac{h_L}{h}\right)\rho_L g \epsilon h \tag{3}$$

$$\rho_G\left(\overline{U} - \bar{u}\right)^2 = \left(1 - \frac{h_L}{D}\right)\frac{\rho_L g \epsilon A}{\mathrm{d}A_L/\mathrm{d}h_L} \tag{4}$$

where A is the area of the pipe, A_L is the area occupied by the liquid and h_L is the height at the middle of the liquid layer. Taitel and Dukler employed geometric arguments to suggest that Eq. (4) predicts a transition to intermittent flow if $h_L/D \geqslant 0.5$ and to annular flow if $h_L/D < 0.5$. The TD approach is now widely used to predict the initiation of intermittent flow, even though understanding of the initiation of slug flow has advanced considerably since 1976.

These recent studies show that the onset of intermittent flow can be defined by one of three criteria: a viscous linear instability of a stratified flow to long wavelength disturbances, a Kelvin–Helmholtz instability of a stratified flow, the stability of a slug. In addition, the observation that the front of a slug is an aerated hydraulic jump can be used to define the transition between a plug flow and a stratified flow. These results have not had as large an impact as they should because a procedure for their implementation has not been developed. The main goal of this work is to address this problem.

A significant outcome is the establishment of the importance of slug stability in predicting transition. Previous work has focused on the instability of a stratified flow. We find that instability of a stratified flow is necessary for slugs to appear, but that it is not a sufficient condition. Slug stability must also be satisfied and, actually, can determine the transition. This is the case for all the systems considered in this paper at relatively high gas velocities. In the two systems with large gas densities, slug stability defines the transition both at high gas velocities and at low gas velocities, where it predicts the initiation of plugs.

All of the stability analyses, including that of Taitel and Dukler, predict a critical h_L/D. Major sources of error in using these results are inaccuracies in the modeling of stratified flows and, in particular, the prediction of the interfacial stress.

2. Review of the literature

An inviscid long wavelength analysis requires that kRe is large, where Re is the Reynolds number and k is a dimensionless wave number. For flow in a channel the inviscid flow assumption breaks down for very long wavelengths. Viscous linear stability analyses have been carried out for small kh and kD by Lin and Hanratty (1986) and by Wu et al. (1987). These analyses need to include the influences of the interfacial stress, τ_i, and the resisting stresses at the wall. They show that because $C \neq \bar{u}$, liquid inertia becomes destabilizing and the critical gas velocity is predicted to be less than what is given by Eq. (1). The most striking confirmation of this theory is a study by Woods et al. (2000) of air and water flowing in a downwardly inclined pipe. Waves are damped at low gas velocities in a declined pipe, so the interfacial stress at transition is easily estimated. This study by Woods and Hanratty provides observations of the appearance of long wavelength waves and their growth into a slug at a gas velocity equal to that predicted by the viscous long wavelength (VLW) analysis. The theory also describes transitions in horizontal air–water flows (Lin and Hanratty, 1986) at low gas velocities, even though slugs are observed to evolve by the bifurcation of small wavelength gravity waves, rather than the growth of very long wavelength waves (Fan et al., 1993). Woods and Hanratty (1996) have argued that, in horizontal stratified flows, a long wavelength instability might be a trigger to enable smaller wavelength waves to evolve into a slug.

Eq. (4) and VLW theory correctly predict that the critical gas velocity for air–water flows will increase with increasing pipe diameter. However, they predict very different effects of liquid viscosity. With increasing viscosity the liquid flow rate decreases for a fixed h_L/D and $\overline{U}$. Consequently, the destabilizing effect of liquid inertia decreases, so that Eqs. (1) and (2) describe the behavior in the limit of very large liquid viscosity.

These considerations motivated a study of the effect of liquid viscosity by Andritsos et al. (1989) in horizontal 9.53 and 2.52 cm pipes. Their measurements agree with VLW theory at viscosities of 16 cp and less. However, quite different results were found for viscosities of 70 and 100 cp. For these conditions, the interface was smooth at transition. For low gas throughputs, the critical gas velocity was found to be independent of pipe diameter and to be given by classical inviscid Kelvin–Helmholtz theory if h_L/D is large enough.

Andritsos and Hanratty (1987a), Lin and Hanratty (1987a,b) and Andreussi and Bendiksen (1989), have observed changes in the wave patterns for a stratified flow. At low gas velocities, waves are generated when the energy fed to the waves by pressure variations in phase with the wave slope is greater than the energy dissipated by liquid viscosity (Cohen and Hanratty, 1965). These waves (which we call Jeffreys waves) will not appear on liquids with large viscosities because dissipative effects become too large. The transmission of energy from the gas to the waves depends on the ratio of the wave velocity to the gas velocity (Miles, 1957; Benjamin, 1959). This dependency could account for the disappearance of Jeffreys waves (1925) in downwardly inclined flows, for which the liquid velocity and the wave velocity increase with increasing declination. When the

gas velocity exceeds the critical value predicted by the classical, inviscid K–H theory, waves are always present in a stratified gas–liquid film. These waves are highly irregular and associated with large interfacial stresses. If the liquid height is large enough, slugs form by wave coalescence (Lin and Hanratty, 1987a,b).

Experiments show that stability analyses of a stratified flow do not describe the transition when h_L/D is small. This observation was considered by TD when they suggested that h_L/D needs to be greater than 0.5. Theoretical understanding of this necessary condition can be obtained by considering the stability of a slug (Ruder et al., 1989; Bendiksen and Espedal, 1992). Dukler and Hubbard (1985) have argued that, for a slug to be stable, the liquid taken up at the front of the slug must be equal to the liquid shed at its back. In a frame of reference moving with the velocity of the front of the slug, V_S, one obtains the following criterion for neutral stability

$$(V_S - \bar{u}_1)A_{L1} = Q_{out} \tag{5}$$

where A_{L1} and $\bar{u}_1$ are, respectively, the cross-sectional area of the liquid layer and the liquid velocity in front of the slug, and Q_{out} is the volumetric flow out of the back of the slug. Eq. (5) defines an area, A_{L1}, in front of the slug, below which a propagating slug decays. Therefore, it is not possible to generate slugs on a stratified flow with A_L less than the critical A_{L1} defined by Eq. (5). Ruder et al. (1989) argued that the back of a slug may be considered to be a bubble. They used the model of a Benjamin bubble (1968) to calculate Q_{out} in the limit of small gas flows. Woods and Hanratty (1996) measured Q_{out} and developed a method to predict the stability of a slug which agrees with observations. The results of Woods and Hanratty are consistent with earlier measurements by Bendiksen (1984) of the motion of long bubbles in inclined tubes. Both Ruder et al. (1989) and Bendiksen and Espedal (1992) have pointed out that for very high gas densities slug stability would determine the transition both at high and at low gas velocities.

Ruder and Hanratty (1990) studied the transition between slug and plug flow. This work and the paper by Ruder et al. (1989) suggest that a necessary condition that requires the front of a slug be a hydraulic jump can be used to define the boundary between slug and plug flows.

3. Theory

3.1. Mean momentum balances

A stratified flow pattern is represented by a simple geometry that represents the liquid flowing along the bottom of the pipe as having a level interface (Fig. 1). The vertical height of the liquid along the centerline is h_L. The length of the interface is S_i. The lengths of the segments of the pipe circumference that are in contact with the gas and with the liquid are S_G and S_L. The areas covered by the gas and the liquid are A_G and A_L. (An overbar is used to refer to time-averaged quantities in Sections 3.2 and 3.3. In Sections 3.1, 3.4, 3.5 and in the figures, time-averages are represented without using of an overbar.) All of the quantities in Fig. 1 can be calculated with geometric relations given by Govier and Aziz (1972), if the pipe diameter and either h_L or A_L are given.

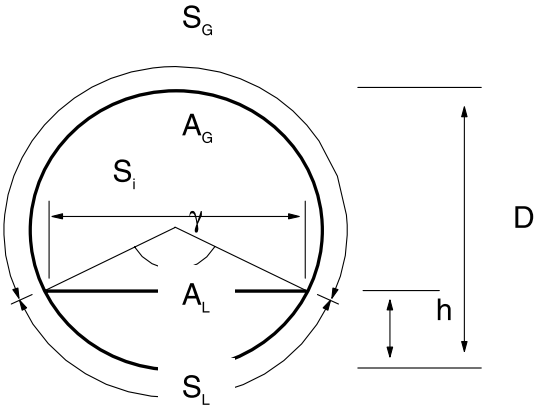

Fig. 1. A simplified geometry for a stratified flow.

The momentum equations are given as

$$A_G \frac{dp}{dx} = -\tau_B S_G - \tau_i S_i + \rho_G A_G g \sin\theta \tag{6}$$

$$A_L \left(\frac{dp}{dx} + \rho_L g \cos\theta \frac{dh_L}{dx} \right) = -\tau_W S_L + \tau_i S_i + \rho_L A_L g \sin\theta \tag{7}$$

Terms ρ_G and ρ_L in Eq. (6) are the gas and liquid densities, θ is the angle of the pipe from the horizontal, dp/dx is the pressure gradient and dh_L/dx is the liquid hydraulic gradient (significant only at very low gas velocities). Stresses τ_B, τ_W represent the resistance at portions of the wall in contact with the gas and the liquid. Term τ_i represents the stress at the interface. The flow is assumed to be fully developed ($dh_L/dx = 0$) or to be varying slowly enough that changes in liquid inertia can be ignored and that pseudo-steady-state assumptions can be made to relate τ_B, τ_i, and τ_W to flow variables.

The liquid and gas phase wall shear stresses, τ_W and τ_B, and the interfacial shear stress, τ_i, are usually defined in terms of friction factors

$$\begin{array}{ll} \tau_B = 1/2 f_B \rho_G U^2 & \tau_W = 1/2 f_W \rho_L u^2 \\ \tau_i = 1/2 f_i \rho_G (U-u)^2 \quad \text{or} & \tau_i = 1/2 f_i \rho_G (U - C_R)^2 \end{array} \tag{8}$$

where U is the average gas velocity, u is the average liquid velocity, and C_R is the wave velocity. In turbulent flows the wall friction factors, f_W and f_B, can be calculated from the Blasius equation if the pipe wall is smooth

$$f_W = 0.0791 Re_L^{-0.25} \qquad f_B = 0.0791 Re_G^{-0.25} \tag{9}$$

The Reynolds numbers are given by

$$Re_L = D_L u / \nu_L \qquad Re_G = D_G U / \nu_G \tag{10}$$

with the hydraulic diameters defined as

$$D_L = 4A_L/S_L \qquad D_G = 4A_G/(S_G + S_i) \tag{11}$$

Table 1
Laminar liquid turbulent gas flow (Russell et al., 1974)

Q^*	h_L/D
1.58×10^{-4}	0.05
8.87×10^{-4}	0.10
4.89×10^{-3}	0.20
1.28×10^{-2}	0.30
2.40×10^{-2}	0.40
3.73×10^{-2}	0.50
5.08×10^{-2}	0.60
6.15×10^{-2}	0.70
6.66×10^{-2}	0.80
6.31×10^{-2}	0.90

In laminar liquid flows with a turbulent gas phase, the friction factor in the liquid phase is not accurately described by a simple function of the Reynolds number. A numerical solution to the liquid phase momentum equation, given by Russell et al. (1974), can be used in place of Eq. (7).

$$\mathrm{d}p/\mathrm{d}x = -(\pi\mu_L U_{SL})/\left(2D^2Q^*\right) \tag{12}$$

Values for Q^* as a function of the non-dimensional liquid height, h_L/D, are given in Table 1.

Andreussi and Bendiksen (1989) and Andritsos and Hanratty (1987a,b) have discussed the accuracy of the relations for τ_W when h_L/D is small. The above equations can be used to calculate the superficial liquid velocity, U_{SL}, if U_{SG}, f_i and A_L (or h_L) are known.

3.2. Kelvin–Helmholtz waves

A theoretical analysis of K–H waves is given by Milne-Thomson (1968) and by Yih (1969). A small amplitude propagating sinusoidal disturbance with wave number $k(k = 2\pi/\lambda)$ is introduced at the interface of a horizontal stratified flow in a channel

$$h = \bar{h} + \hat{h}\exp\left[\mathrm{i}k(x - Ct)\right] \tag{13}$$

where $\bar{h}$ is the average height of the liquid, $\hat{h}$ is the amplitude of the disturbance, and C is the wave velocity. The gas and liquid layers are assumed to be inviscid and to have uniform mean velocities. A consideration of the linear momentum equations for the gas and the liquid produces the following dispersion relation:

$$k\rho_L(\bar{u} - C)^2 \coth k\bar{h} + k\rho_G\left(\overline{U} - C\right)^2 \coth k\overline{H} = g\cos\theta(\rho_L - \rho_G) + \sigma k^2 \tag{14}$$

Here $\overline{H}$ is the average height of the gas, σ is the surface tension, and g is the acceleration of gravity. The wave velocity, C, is complex with $C = C_R + \mathrm{i}C_I$. Solving Eq. (14) for the conditions at which $C_I = 0$ results in relations for neutral stability (or the onset of instability) of a stratified flow

$$(\overline{U} - \bar{u})^2 = [(g/k)\cos\theta(\rho_L - \rho_G)/\rho_G + \sigma k/\rho_G]\left[\tanh\left(k\overline{H}\right) + \rho_G/\rho_L \tanh(k\bar{h})\right] \tag{15}$$

$$C_R = \frac{\rho_G \overline{U} \tanh\left(k\bar{h}\right) + \rho_L \bar{u} \tanh\left(k\overline{H}\right)}{\rho_L \tanh\left(k\overline{H}\right) + \rho_G \tanh\left(k\bar{h}\right)} \tag{16}$$

Eqs. (15) and (16) simplify if the gas is deep $\left(\tanh\left(k\overline{H}\right) = 1\right)$ and the liquid density is much greater than the gas density $(\rho_G \ll \rho_L)$

$$\left(\overline{U} - \bar{u}\right)^2 = (g/k)\cos\theta(\rho_L/\rho_G) + \sigma k/\rho_G \tag{17}$$

$$C_R = \bar{u} \tag{18}$$

The minimum relative velocity at which Eq. (17) is satisfied gives a critical relative gas velocity and a critical wavenumber,

$$k_{Crit} = \left(\rho_L g \cos\theta/\sigma\right)^{0.5} \tag{19a}$$

$$\left(\overline{U} - \bar{u}\right)^2_{Crit} = 2\left(\frac{\sigma g \cos\theta}{\rho_L}\right)^{0.5} \frac{\rho_L}{\rho_G} \tag{19b}$$

The critical relative velocity predicted for flow in a channel is a close approximation to the critical relative velocity for a stratified flow in a round pipe. For air and water at atmospheric pressure, Eqs. (17) and (18) predict instability to occur at $\left(\overline{U} - \bar{u}\right)_{Crit} = 6.6$ m/s and $\lambda = 1.7$ cm. Increasing the gas density or lowering the surface tension will result in lower critical gas velocities. This is the case for high pressure natural gas condensate flows where K - H waves are predicted to appear at $\left(\overline{U} - \bar{u}\right)_{Crit} = 0.54$ m/s and $\lambda = 0.8$ cm.

When a deep gas assumption is not valid $\left(\tanh\left(k\overline{H}\right) \neq 1 \text{ and } \rho_G \ll \rho_L\right)$, Eq. (15) gives

$$\left(\overline{U} - \bar{u}\right)^2 = \left[(g/k)\cos\theta\rho_L/\rho_G + \sigma k/\rho_G\right]\tanh\left(k\overline{H}\right) \tag{20}$$

This is applicable to thick liquid layers in small diameter pipes. With $\tanh\left(k\overline{H}\right) < 1$, Eq. (20) predicts the onset of K–H waves at a lower gas velocity than is given by Eqs. (17) and (18). In the limit of small $k\overline{H}$, Eq. (20) gives Eq. (1) for a horizontal channel since surface tension effects would be negligible.

3.3. Viscous long wavelength instability

The VLW analyses of Lin and Hanratty (1986) and of Wu et al. (1987) are essentially the same as was used by Hanratty and Hershman (1961) to describe waves on thin films over which air is blowing. Integral forms of the equations of motion are used and the pressure is assumed to vary only because of gravity in a direction perpendicular to the direction of mean flow. Thus, the equations of conservation of mass and momentum in the liquid are given as

$$\frac{\partial A_L}{\partial t} + \frac{\partial(uA_L)}{\partial x} = 0 \tag{21}$$

$$\frac{\partial(uA_L)}{\partial t} + \frac{\partial(u^2 A_L)}{\partial x} = -\frac{A_L}{\rho_L}\left(\frac{\partial P_i}{\partial x} + \rho_L g \cos\theta \frac{\partial h}{\partial x}\right) + \frac{1}{\rho_L}\left(\tau_i S_i - \tau_W S_L\right) + A_L g \sin\theta \tag{22}$$

where P_i is the gas phase pressure at the interface, τ_i, the shear stress at the interface and τ_W, the resisting stress at the wall.

The quantities in this equation are assumed to be given by the sum of mean and fluctuating contributions. Thus

$$A_{\mathrm{L}} = \overline{A}_{\mathrm{L}} + \hat{A}_{\mathrm{L}} \exp\left[\mathrm{i}k(x - Ct)\right] \tag{23}$$

where k is the wavenumber, C is the complex wave velocity and $\hat{A}_{\mathrm{L}}$ is a real number which is the amplitude of the disturbance. The amplitudes of the wave-induced variations of the pressure and of the resisting stresses are complex

$$\begin{aligned} \hat{P}_{\mathrm{i}} &= \hat{P}_{\mathrm{iR}} + \mathrm{i}\hat{P}_{\mathrm{iI}} \\ \hat{\tau}_{\mathrm{W}} &= \hat{\tau}_{\mathrm{WR}} + \mathrm{i}\hat{\tau}_{\mathrm{WI}} \\ \hat{\tau}_{\mathrm{i}} &= \hat{\tau}_{\mathrm{iR}} + \mathrm{i}\tau_{\mathrm{iI}} \end{aligned} \tag{24}$$

Eq. (21) gives a relation between the amplitude of the fluctuations in the liquid velocity, $\hat{u}$, and $\hat{A}_{\mathrm{L}}$.

$$\hat{u} = (C - \bar{u})\frac{\hat{A}_{\mathrm{L}}}{\overline{A}_{\mathrm{L}}} \tag{25}$$

If equations of the form of Eq. (23) are substituted into Eq. (22) and non-linear terms in the fluctuating quantities are ignored, a relation for $C = C_{\mathrm{R}} + \mathrm{i}C_{\mathrm{i}}$ is obtained. The real and imaginary parts of this equation yield the following if neutral stability ($C_{\mathrm{i}} = 0$) is assumed:

$$-\left(\frac{C_{\mathrm{R}}}{\bar{u}} - 1\right)^2 = -\frac{\overline{A}_{\mathrm{L}}}{\rho_{\mathrm{L}}\bar{u}^2}\frac{\hat{P}_{\mathrm{iR}}}{\hat{A}_{\mathrm{L}}} - \frac{g\overline{A}_{\mathrm{L}}\cos\theta}{\bar{u}^2}\frac{\hat{h}}{\hat{A}_{\mathrm{L}}} + \frac{\overline{S}_{\mathrm{i}}}{k\rho_{\mathrm{L}}\bar{u}^2}\frac{\hat{\tau}_{\mathrm{iI}}}{\hat{A}_{\mathrm{L}}} - \frac{\overline{S}_{\mathrm{L}}}{k\rho_{\mathrm{L}}\bar{u}^2}\frac{\hat{\tau}_{\mathrm{WI}}}{\hat{A}_{\mathrm{L}}} \tag{26}$$

$$0 = \overline{A}_{\mathrm{L}}k\frac{\hat{P}_{\mathrm{iI}}}{\hat{A}_{\mathrm{L}}} + \frac{\bar{\tau}_{\mathrm{W}}\overline{S}_{\mathrm{L}}}{\overline{A}_{\mathrm{L}}} - \frac{\bar{\tau}_{\mathrm{i}}\overline{S}_{\mathrm{i}}}{\overline{A}_{\mathrm{L}}} + \overline{S}_{\mathrm{i}}\frac{\hat{\tau}_{\mathrm{iR}}}{\hat{A}_{\mathrm{L}}} - \overline{S}_{\mathrm{L}}\frac{\hat{\tau}_{\mathrm{WR}}}{\hat{A}_{\mathrm{L}}} + \bar{\tau}_{\mathrm{i}}\frac{\hat{S}_{\mathrm{i}}}{\hat{A}_{\mathrm{L}}} - \bar{\tau}_{\mathrm{W}}\frac{\hat{S}_{\mathrm{L}}}{\hat{A}_{\mathrm{L}}} \tag{27}$$

Terms $\hat{P}_{\mathrm{iR}}$ and $\hat{P}_{\mathrm{iI}}$ are evaluated by considering a linearized version of the integral forms of the equations of conservation of mass and momentum for the gas phase. These introduce a resisting stress on the gas flow at the wall, τ_{B}. Eq. (26) gives the following relation for the range of conditions considered in this paper

$$0 = \rho_{\mathrm{L}}(C_{\mathrm{R}} - \bar{u})^2 + \frac{\overline{A}_{\mathrm{L}}}{\overline{A}_{\mathrm{G}}}\rho_{\mathrm{G}}\left(\overline{U} - C_{\mathrm{R}}\right)^2 - g\overline{A}_{\mathrm{L}}\rho_{\mathrm{L}}\cos\theta\frac{\hat{h}}{\hat{A}_{\mathrm{L}}} \tag{28}$$

where $\left(\overline{U} - C_{\mathrm{R}}\right) \cong \overline{U}$ and $(\hat{A}_{\mathrm{L}}/\hat{h}) = \mathrm{d}A_{\mathrm{L}}/\mathrm{d}h$. Eq. (28) defines a critical gas velocity for the initiation of a long wavelength disturbance. The first term represents the destabilizing effect of liquid inertia and the third, the stabilizing effect of gravity. For an inviscid flow, $C_{\mathrm{R}} = \bar{u}$ and liquid inertia has no influence. However, for very long wavelength waves the stresses, τ_{i}, τ_{W} and τ_{B} need to be considered in order to obtain a wave velocity to substitute into Eq. (28). The wave velocity, C_{R}, in Eq. (28) is calculated from Eq. (27). Wave velocities obtained in this way are the kinematic waves defined by Lighthill and Whitham (1955).

The terms $\hat{\tau}_{\mathrm{iR}}$, $\hat{\tau}_{\mathrm{WR}}$, and $\hat{\tau}_{\mathrm{BR}}$ are obtained by making the pseudo-steady-state assumption, that the same relation for τ_{i}, τ_{W}, and τ_{B} are valid both for the disturbed and undisturbed flows. Solving Eqs. (8)–(11) for the fluctuating shear stresses gives

$$\frac{\hat{\tau}_{WR}}{\bar{\tau}_W} = 1.75\left(\frac{C_R}{\bar{u}_L}\right)\frac{\hat{A}_L}{\overline{A}_L} - 2\frac{\hat{A}_L}{\overline{A}_L} + \frac{1}{4}\frac{\hat{S}_L}{\overline{S}_L} \tag{29}$$

$$\frac{\hat{\tau}_{BR}}{\bar{\tau}_B} = 2\frac{\hat{A}_L}{A - \overline{A}_L} + \frac{1}{4}\frac{\hat{S}_G + \hat{S}_i}{\overline{S}_G + \overline{S}_i} \tag{30}$$

$$\frac{\hat{\tau}_{iR}}{\bar{\tau}_i} = 2\frac{\hat{A}_L}{A - \overline{A}_L} + \frac{\hat{f}_i}{\overline{f}_i} \tag{31}$$

$$\frac{\hat{\tau}_{WI}}{\bar{\tau}_W} = 0 \qquad \frac{\hat{\tau}_{BI}}{\bar{\tau}_B} = 0 \qquad \frac{\hat{\tau}_{iI}}{\bar{\tau}_i} = 0 \tag{32}$$

Lin and Hanratty (1986) derived an expression for $\hat{f}_i$ in Eq. (31) by assuming f_i is a function of the liquid Reynolds number. Measurements of the interfacial friction factor taken by Simmons and Hanratty (2001) suggest that the friction factor is roughly constant at low velocity. With $\hat{f}_i = 0$, Eq. (31) simplifies to

$$\frac{\hat{\tau}_{iR}}{\bar{\tau}_i} = 2\frac{\hat{A}_L}{A - \overline{A}_L} \tag{33}$$

Details of the above analysis are found in Lin and Hanratty (1986).

3.4. Slug stability

Typical features of a slug are shown in Fig. 2. The front is traveling downstream at a velocity V_s. It scoops up slower moving fluid ($V_s > u_1$) from the liquid layer in front at a volumetric flow rate Q_{in}. The liquid in the slug at station 3 is traveling at an average velocity u_3. The rear of the slug travels at the bubble velocity, V_B. Since V_B is greater than u_3, liquid is shed out of the tail at a volumetric flow rate Q_{out}. If the mixture velocity, ($U_{Mix} = U_{SG} + U_{SL}$), is large enough, the slug will be aerated by small bubbles traveling at an average velocity U_3. The volume occupied by bubbles in the slug is represented by the void fraction, ε.

In a reference frame translating at velocity V_s, the volumetric flow rates of liquid entering the front of the slug and leaving the back are given by

$$Q_{in} = (V_s - u_1)A_{L1} \tag{34}$$

$$Q_{out} = (V_B - u_3)(1 - \varepsilon)A \tag{35}$$

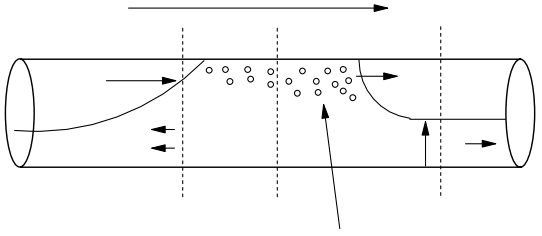

Fig. 2. Slug flow parameters.

When the volumetric flow rates in and out of the slug are unequal the slug will either grow ($Q_{out} < Q_{in}$) or decay ($Q_{out} > Q_{in}$). When Q_{out} is equal to Q_{in} the slug is neutrally stable and $V_s = V_B$. Eqs. (34) and (35) give the following condition for A_{L1} for a slug which is neither growing nor decaying:

$$(A_{L1}/A)_{Crit} = (V_B - u_3)(1 - \varepsilon)/(V_B - u_1) \tag{36}$$

This differs from Eq. (5) in that V_B, rather than Q_{out}, is modeled. That is, Q_{out} is defined in terms of V_B. The use of Eq. (36), to calculate $(A_{L1}/A)_{Crit}$, requires relations for u_3, ε, and V_B.

3.4.1. Relations for u_3 and ε

Assuming incompressible flow, a volume balance between the inlet of the pipe and station 3 gives

$$U_{SG} + U_{SL} = \varepsilon U_3 + (1 - \varepsilon)u_3 \tag{37}$$

Introducing a slip ratio, $s = U_3/u_3$, the velocity of the liquid at station 3 can be written as

$$u_3 = U_{Mix}/(1 + (s - 1)\varepsilon) \tag{38}$$

The void fraction in the slug, ε, has been measured or analyzed by several researchers (Woods and Hanratty, 1996; Bendiksen, 1984; Andreussi and Bendiksen, 1989; Nydal et al., 1992). For $U_{Mix} < 2\sqrt{gD}$ it is negligible. For $U_{Mix} > 2\sqrt{gD}$ the data of Woods (Woods, 1998; Woods and Hanratty, 1996) can be correlated by the expression

$$\varepsilon = 0.8\left[1 - \frac{1}{\left(1 + (U_{Mix}/8.66)^{1.39}\right)}\right] \tag{39}$$

The slip ratio, s, was estimated indirectly in experiments by Woods and Hanratty (1996) for air–water flows. From this study $s = 1$ for $U_{Mix} < 4$ m/s and $s = 1.3$–1.5 for $U_{Mix} > 4$ m/s.

3.4.2. Bubble velocity

The bubble velocity has been measured over a wide range of pipe diameters in studies by Ruder and Hanratty (1990), Woods et al., (1996), Gregory and Scott (1969), Kouba and Jepson (1990), and Nydal et al. (1992). Bendiksen (1984), who looked at the velocity of bubbles injected into a moving liquid stream, defined three regimes.

At low mixture velocities ($U_{Mix} < 2\sqrt{gD}$) gravitational effects are important and the back of the slug or plug can be modeled as a Benjamin bubble (Benjamin, 1968). The shedding from the tail is then given as

$$Q_{out} = 0.542A\sqrt{gD} \tag{40}$$

At the low mixture velocities, where Eq. (40) is applicable, aeration is negligible. For $\varepsilon = 0$ conservation of volume for an incompressible flow Eq. (37) gives

$$u_3 = U_{Mix} \tag{41}$$

From Eqs. (38), (40) and (41) one finds that

$$V_B = U_{Mix} + 0.542\sqrt{gD} \quad U_{Mix} < 2\sqrt{gD} \tag{42}$$

At slightly higher mixture velocities ($2\sqrt{gD} < U_{Mix} < 3.5\sqrt{gD}$) both inertial and gravitational effects are important. In this range, the experimental data of Bendiksen (1984) and of Woods and Hanratty (1996) give

$$V_B = 1.1U_{Mix} + 0.542\sqrt{gD} \quad 2\sqrt{gD} < U_{Mix} < 3.5\sqrt{gD} \tag{43}$$

At higher mixture velocities ($U_{Mix} > 3.5\sqrt{gD}$) inertia dominates; the bubble velocity is given by Woods and Hanratty (1996) as

$$V_B = 1.2U_{Mix} \quad U_{Mix} > 3.5\sqrt{gD} \tag{44}$$

The above relations were established for mixture Reynolds numbers $\left(Re_{U_{Mix}} = U_{Mix}D/\nu_L\right)$ well above 2300. Sam and Crowley (1986) measured slug velocities in glycerin–water solutions flowing with air for $Re_{U_{Mix}} < 2300$ and found, for these laminar slugs, that

$$V_B = 2U_{Mix} \tag{45}$$

3.4.3. Calculation of the stability height

Eqs. (36), (38), (32), and the bubble velocity relations Eqs. (42)–(45) can be used to predict the liquid layer height needed for stable slugs to exist $(A_{L1}/A)_{Crit}$. The slip ratio, s, is assumed equal to 1 for $U_{Mix} < 3.5\sqrt{gD}$. The magnitude of the interfacial friction factor depends on the wave activity at the interface. The ratio of the interfacial friction factor to the value that would exist if the surface were smooth, f_i/f_s, can vary from 2 to 25. It must be found, experimentally, for the conditions of interest if an accurate prediction of U_{SL} from $(A_{L1}/A)_{Crit}$ is to be obtained.

3.5. Slug/plug boundary

Ruder and Hanratty (1990) studied plug flows for air and water flowing in a 9.53 cm horizontal pipe and found that a symmetric bubble exists at $Fr = (V_s - u_1)/\sqrt{gD} \cong 1.2$. For $1.2 < Fr < 1.8$ the back of the slug was observed to maintain a shedding rate given by Eq. (40) and the front was observed to contain a hydraulic jump. For $Fr < 1.2$ the bubble can be asymmetric. We have selected $Fr = 1.2$ as a criterion for the transition from slug flow to plug flow. From Eqs. (6), (40) and the assumption of a critical Fr of 1.2, one obtains a critical A_{L1} given by

$$(A_{L1}/A)_{Crit} \cong 0.45 \tag{46}$$

A mass balance can be written for each phase in terms of the intermittency, I, defined as the fraction of time a stationary probe in the flow would remain in contact with a slug:

$$AU_{SL} = (1 - I)u_1A_{L1} + IU_{Mix}A \tag{47}$$

$$AU_{SG} = (1 - I)U_1(A - A_{L1}) \tag{48}$$

The velocity of the gas flowing over the stratified flow in front of the slug, U_1, can be found by applying conservation of mass to the gas flow. For an unaerated slug this gives

$$U_1 = V_s \tag{49}$$

By adding Eqs. (47) and (48) and using Eqs. (46) and (49) one calculates a mixture velocity which corresponds to $Fr \cong 1.2$.

$$U_{\mathrm{Mix}} \cong 0.66\sqrt{gD} + u_1 \tag{50}$$

The velocity of the liquid in the stratified flow, u_1, can be evaluated by solving the gas and liquid momentum balances, Eqs. (6) and (7), with the height of the liquid layer given by Eq. (46). The hydraulic gradient, $\mathrm{d}h/\mathrm{d}x$, in addition to the drag at the interface are needed for an accurate estimate of u_1.

4. Experiments

The data that will be used to examine theoretical predictions demonstrate the effects of pipe diameter, liquid viscosity, downward inclinations, gas density, and surface tension on the transition from stratified to slug and plug flow. System properties are summarized in Table 2.

Andritsos et al. (1989) observed transitions in a 25 m long horizontal pipe with a diameter of 9.53 cm for air and liquids with viscosities of 1 cp (water) and 100 cp (glycerin–water solution). Andritsos and Hanratty (1987a) studied transitions in a 10 m long horizontal pipe with $D = 2.52$ cm for air and liquids with viscosities of 1 cp (water) and 70 cp (glycerin–water solution). Woods et al. (2000) studied air and water flowing in a pipe with $D = 7.63$ cm, a length of 23 m, and an inclination of $-0.5°$. In all of these investigations the thickness of the liquid layer, h_L, was measured at several locations along the pipe by pairs of parallel wire conductance probes which extend vertically across the pipe cross-section.

Heights of the liquid layer, h_L, and the superficial liquid velocity at transition to an intermittent flow are plotted in Fig. 3. A striking feature is the large range of critical U_{SL}, compared to critical h_L/D. This emphasizes the importance of being able to solve the average momentum equations for a stratified flow to obtain U_{SL} if h_L/D and U_{SG} are known.

An important feature of Fig. 3 is that the h_L/D and U_{SL} required for transition in air–water flows in a horizontal pipe increase with pipe diameter at low U_{SG}. They are roughly independent of pipe diameter at large U_{SG} where slugs form by coalescence of small wavelength irregular waves that have evolved from a Kelvin–Helmholtz instability. When the pipe is inclined downward the gravitational pull causes larger liquid velocities (at the same h_L/D). This accounts for the increase in U_{SL} required for transition that is shown in Fig. 3. At large U_{SG}, the gravitational pull on the liquid becomes less important, compared to the gas drag at the interface, so that transitions in horizontal pipes and pipes inclined at $\theta = -0.5°$ are approximately the same. A consideration of

Table 2
Summary of system properties

	Air–water	Air–glycerin/water	Natural gas	Freon–water
Pipe diameter (cm)	9.53, 7.63, 2.52	9.53, 2.52	20.3	17.8
Gas density (kg/m^3)	1.2	1.2	65	32.5
Pressure (bar)	1	1	75	5.5
Liquid density (kg/m^3)	1000	1220	720	1000
Gas viscosity (kg/ms)	1.8×10^{-5}	1.8×10^{-5}	1×10^{-5}	1.3×10^{-5}
Liquid viscosity (kg/ms)	0.001	0.1, 0.07	0.00055	0.001
Interfacial tension (N/m)	0.07	0.066	0.0118	0.07

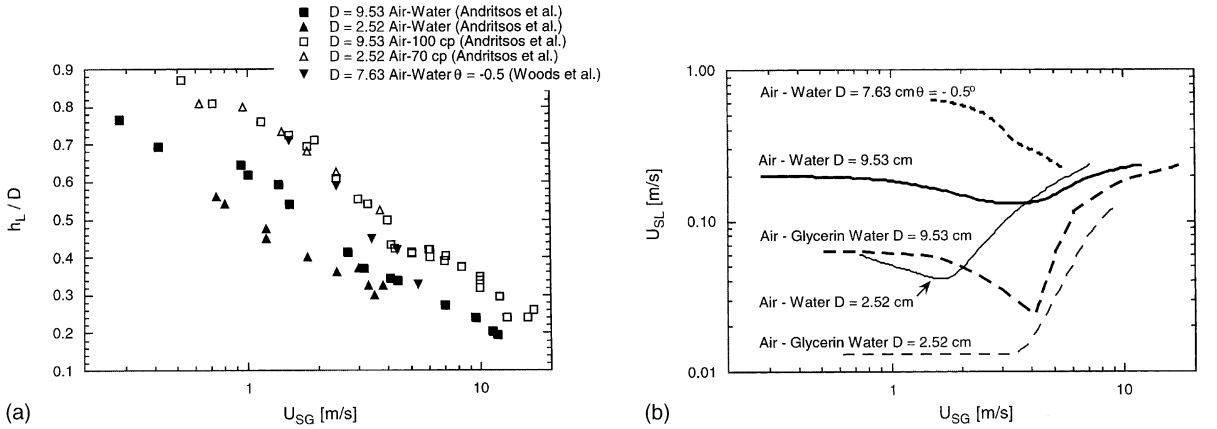

Fig. 3. Flow regime transition data at ambient pressure: (a) critical h/D (b) critical U_{SL}.

the critical h_L/D (rather than the critical U_{SL}) shows that downward inclinations cause a stabilization in that transition occurs at a larger h_L/D.

An increase in liquid viscosity increases the stability; that is, transition occurs at higher h_L/D. The independence of the critical h_L/D of pipe diameter at low gas velocities is indicative of a difference in the instability mechanisms for flows with low and high liquid viscosities. The lower critical U_{SL} for high liquid viscosities reflects the increased resistance of the wall to the liquid flow for a given h_L/D and U_{SL} for laminar flows. At high gas velocities the critical h_L/D is smaller than for low gas velocities, the liquid flow is turbulent at transition, and the critical U_{SL} and h_L/D become approximately independent of pipe diameter and of liquid viscosity.

Wu et al. (1987) reported results on transitions in a 218 m long, horizontal 20.3 cm pipe for natural gas/condensate flowing at a high pressure ($\rho_G \cong 65$ kg/m^3 and $\sigma \cong 0.0118$ N/m). Measurements of the height of the liquid layer at transition were not reported. The critical superficial liquid velocities are shown in Fig. 4.

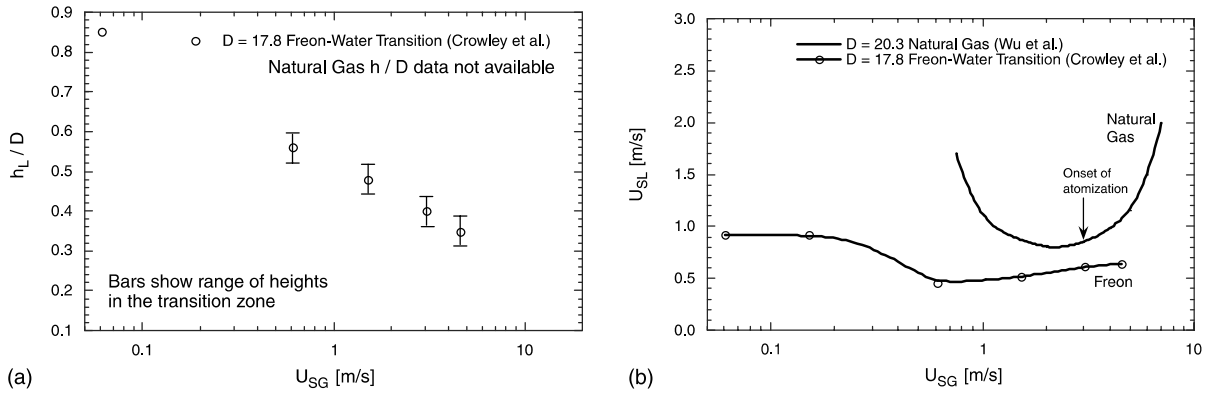

Fig. 4. Flow regime transition data at high gas density.

Crowley et al. (1986) observed transitions in a 34 m long horizontal 17.8 cm diameter pipe for the flow of high pressure Freon gas ($\rho_G = 32.5$ kg/m^3) and water. Measurements of the height of the liquid layer were obtained using a rake of conductivity probes. The spacing between the conductivity sensors allowed h_L/D measurements to an accuracy of $\pm 4\%$. The heights of the liquid layer, h_L, and the superficial liquid velocity, U_{SL}, at transition are presented as a function of the superficial gas velocity, U_{SG}, in Fig. 4.

5. Interpretation of experiments

5.1. Outline

An analysis of the results discussed in Section 4 supports the observation that a number of different mechanisms are responsible for the transition from stratified to slug or plug flow. The specific mechanism, that is applicable, is found to depend on which instability theory predicts the lowest critical h_L/D at a given U_{SG}, and whether the height of the liquid layer is large enough to maintain a stable slug.

Predictions of the critical height of the liquid layer are made using Kelvin–Helmholtz theory, Eqs. (17), (19a) and (19b) VLW theory, Eqs. (27) and (28), and slug stability theory, Eq. (36). The critical superficial liquid velocity is calculated from the critical height by using the liquid and gas phase momentum balances, Eqs. (6) and (7), for turbulent liquid/turbulent gas flows and Eqs. (6) and (12) for laminar liquid/turbulent gas flows. Predictions of the superficial liquid velocity at the boundary between plug and slug flow are made by using Eq. (50).

5.2. Interfacial friction factors

Because of the presence of waves, the interfacial friction factor, f_i, can be larger than the friction factor for a smooth surface, f_s. It has been correlated with some success by Andritsos and Hanratty (1987b) as $f_i/f_s = f(\Delta h/\lambda)$, where Δh is the wave height and λ is the wavelength. However, no relation for f_i/f_s, that applies over a large range of fluid properties and flow conditions, is presently available. The interfacial friction factor plays a critical role in the prediction of transition since it is needed to calculate U_{SL}. In the VLW and slug stability theories it is needed to predict the critical h_L/D.

Measurements of the interfacial friction factor were made by Andritsos and Hanratty (1987b) for the flow of air and water and of air and glycerin–water solutions in 9.53 and 2.52 cm horizontal pipes. A general correlation was developed from this work for gas velocities above the critical velocity needed for a K–H instability to occur, $\overline{U}_{Crit}$. Bontozoglu and Hanratty (1989) restated this correlation, accounting for the relative velocity between the gas and the liquid; that is, $\overline{U}_{Crit}$ is replaced by $\left(\overline{U} - \bar{u}\right)_{Crit}$. Simmons and Hanratty (2001) measured f_i/f_s for the flow of air and water in a 7.63 cm pipe at flow conditions near transition for gas velocities less than $\left(\overline{U} - \bar{u}\right)_{Crit}$.

These works suggest that interfacial friction factors close to transition can be estimated for air and water and air and water–glycerin flows from the following relations:

$$f_i/f_s = 2 \quad \text{smooth liquid surface} \quad (\overline{U} - \bar{u}) \leqslant (\overline{U} - \bar{u})_{\text{Crit}} \tag{51}$$

$$f_i/f_s = 5 \quad \text{wavy liquid surface} \quad (\overline{U} - \bar{u}) \leqslant (\overline{U} - \bar{u})_{\text{Crit}} \tag{52}$$

$$f_i/f_s = 5 + 15(h/d)^{0.5}\left[(\overline{U} - \bar{u})/(\overline{U} - \bar{u})_{\text{Crit}} - 1\right] \quad (\overline{U} - \bar{u}) > (\overline{U} - \bar{u})_{\text{Crit}} \tag{53}$$

Eq. (51) follows from results presented by Andritsos and Hanratty (1987b). Eq. (52) is an average value from data taken by Simmons and Hanratty (2001). Eq. (53) is a correlation given by Bontozoglu and Hanratty (1989), modified so as to be continuous when switching between Eqs. (52) and (53).

Crowley et al. (1986) measured interfacial friction factors for flows of Freon gas and water in a horizontal 17.8 cm pipe. At high gas velocities (for flow conditions near transition), f_i/f_s was found to be on the order of 15–20. At low gas velocities, no interfacial friction data are reported for conditions near transition. Interfacial friction factors are estimated for high pressure flows by using the following relations:

$$f_i/f_s = 2 \quad (\overline{U} - \bar{u}) \leqslant (\overline{U} - \bar{u})_{\text{Crit}} \tag{54}$$

$$f_i/f_s = 15 \quad (\overline{U} - \bar{u}) > (\overline{U} - \bar{u})_{\text{Crit}} \tag{55}$$

5.3. Comparison between theory and experiments for air–water flow in horizontal pipes

Figs. 5 and 6 compare theoretical predictions of the critical h_L/D and U_{SL} using Kelvin–Helmholtz theory, viscous long wavelength theory, and slug stability theory with measurements for air and water flowing in a horizontal pipe. Plug/slug boundary predictions are also shown for $I < 0.5$. Friction factors were estimated using Eqs. (52) and (53). Hydraulic gradients were estimated using data obtained by Andritsos et al. (1989) in a 9.53 cm pipe ($dh/dx = -0.0005$ for $U_{SG} < 3$ m/s). In the slug stability calcuations, $s = 1$ for $U_{Mix} \leqslant 3.5\sqrt{gD}$ and $s = 1.3$ for

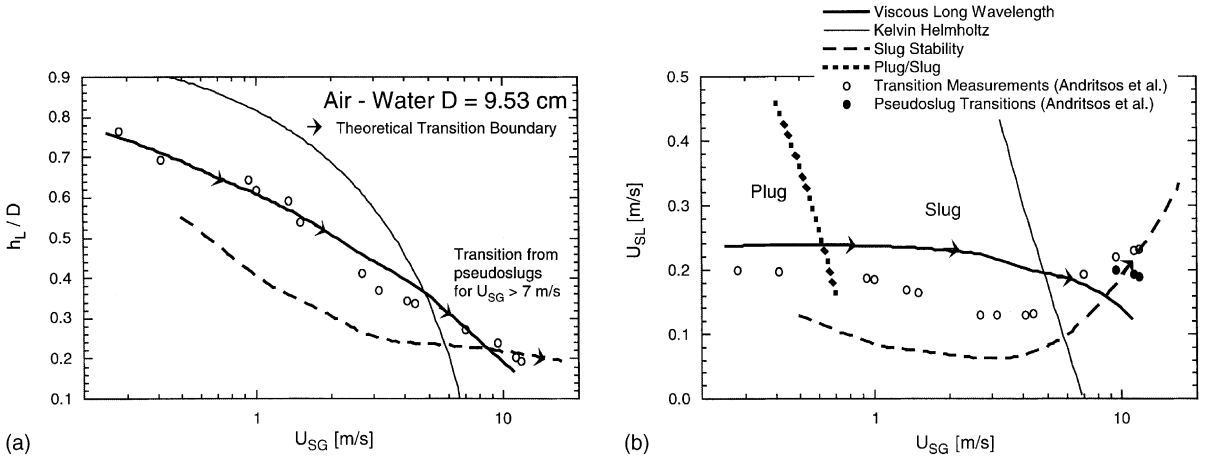

Fig. 5. Air–water theoretical predictions and transition data, $D = 9.53$ cm.

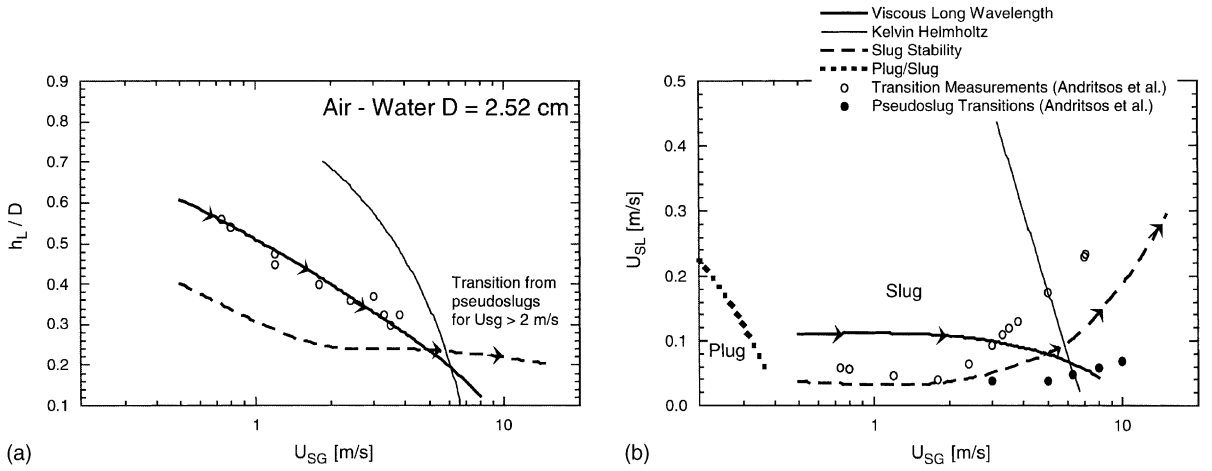

Fig. 6. Air–water theoretical predictions and transition data, $D = 2.52$ cm.

$U_{Mix} > 3.5\sqrt{gD}$. The void fraction was calculated using Eq. (39). Arrows are used to indicate the proposed transition boundary.

Good agreement is observed at small U_{SG} between the observed critical h_L/D and the VLW analysis. Furthermore, transition occurs above the h_L/D required for the formation of stable slugs. For large U_{SG} the h_L/D required for a stable slug is larger than the prediction from the VLW analysis and from Kelvin–Helmholtz theory. Consequently, this instability should determine the transition to a slug flow. The measurements of critical h_L/D for $D = 9.53$ cm are consistent with this proposal. Calculations of critical h_L/D are not sensitive to the choice of f_i/f_s. This is not the case for calculations of the critical U_{SL}. For example, a threefold change of f_i/f_s in applying VLW to air–water flow in a 9.53 cm pipe caused a twofold variation of the predicted critical liquid flow and a negligible variation in the predicted critical liquid height. The agreement between the critical U_{SL} with measurements is not so good. This reflects inaccuracies in estimating f_i/f_s.

In the 9.53 cm pipe, plug flow is predicted to occur for $U_{SG} < 0.7$ m/s at $U_{SL} = 0.15$ m/s and at slightly lower U_{SG} as U_{SL} increases. Lower critical U_{SG} for a transition from slug flow to plug flow are predicted for the 2.52 cm pipe.

Visual observations show that, at large U_{SG}, the K–H instability leads to the formation of irregular waves if h_L/D is below that required for slug stability.

Lin and Hanratty (1987a,b) observed a pseudo-slug region in which highly aerated waves are observed to bridge the whole pipe cross-section. These are differentiated from slugs in that they have smaller velocities, are accompanied by smaller pressure pulses and are not coherent over long distances in the pipeline. The filled points in Figs. 5 and 6 represent a transition from stratified flow to a flow with pseudo-slugs.

5.4. Air and glycerin–water solutions in horizontal pipes

Theoretical calculations of critical h_L/D and U_{SL} are compared with measurements for the flow of air and glycerin–water solutions in Figs. 7 and 8. Predictions with VLW theory are not shown

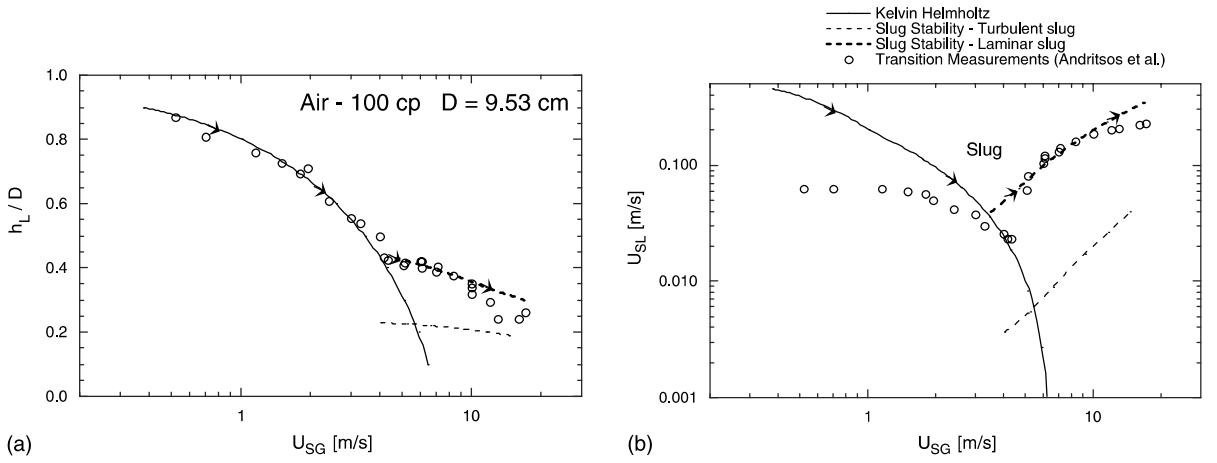

Fig. 7. Air–100 cp glycerin–water solution theoretical predictions and transition data, $D = 9.53$ cm.

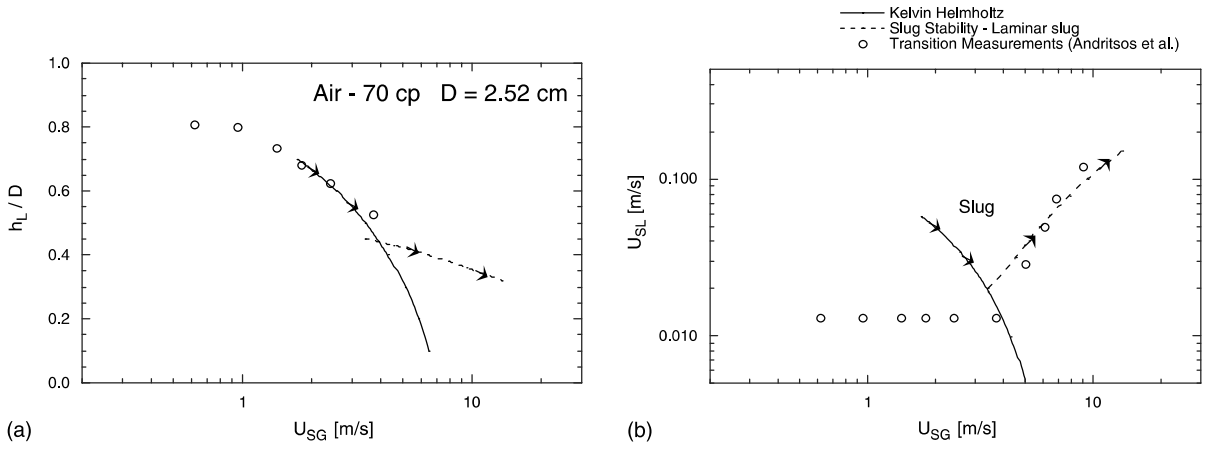

Fig. 8. Air–70 cp glycerin–water solution theoretical predictions and transition, $D = 2.52$ cm.

as neither these waves nor Jeffreys waves (Cohen and Hanratty, 1965) were found to occur in flows of liquids with high viscosities (Andritsos et al., 1989). Friction factors were estimated by using Eq. (51) in the K–H calculations and by using Eq. (53) in the slug stability calculations. Due to the high liquid viscosity, the relation for a laminar bubble, Eq. (45), was used to calculate the shedding rate needed to consider slug stability. Eq. (12) was used instead of Eq. (9). The slip ratio was assumed to be equal to 1.3 and Eq. (39) was used to calculate the void fraction.

Critical h_L/D for a 100 cp liquid flowing in a 9.53 cm pipe agree with predictions from K–H theory for $U_{SG} < 4$ m/s. For $U_{SG} > 4$ m/s, transition was visually observed to be due to the coalescence of K–H waves; predictions from slug stability theory agree with the transition data. Since the mixture Reynolds number reaches 10,000 at $U_{SG} \sim 10$ m/s, the flow might be expected to be turbulent. Predictions of slug stability using bubble velocity relations for both turbulent, Eqs. (42)–(44) and laminar, Eq. (45), flows are shown in Fig. 7.

Critical h_L/D for a 70 cp liquid flowing in a 2.52 cm pipe agree with predictions from K–H theory if $U_{SG} \leqslant 3$ m/s. For $U_{SG} > 4$ m/s, critical heights of the liquid layer were not reported. The observed U_{SL} at transition for $U_{SG} > 4$ m/s show a trend similar to that predicted by slug stability theory. The mixture Reynolds number reaches 3000 at a $U_{SG} \sim 10$ m/s. Slug stability calculations could require the use of relations for bubble velocity in turbulent fluids at higher U_{SG} than were studied.

Critical U_{SL} do not agree with predictions for $U_{SG} < 4$ m/s in both the 100 and 70 cp flows. Better agreement would be expected since theoretical and experimental values of h_L/D are close to one another. This suggests either that incorrect hydraulic gradients are used or that the equation for the liquid flow is not appropriate.

It is noted that the critical h_L/D for the 2.52 and 9.53 cm pipes are the same at these high viscosities. This is contrary to the prediction of a strong effect of pipe diameter in the Taitel and Dukler correlation, but is consistent with defining transition as due to a K–H instability.

5.5. Predictions for declined flow of air and water

Measurements of the critical h_L/D and U_{SL} are compared in Fig. 9 for the flow of air and water in a 7.63 cm pipe that is inclined at $-0.5°$. In the VLW and K–H calculations, f_i/f_s was assumed to be given by Eq. (51) as a smooth surface was observed in these flows. In the slug stability calculations, $s = 1$ for $U_{Mix} \leqslant 3.5\sqrt{gD}$ and $s = 1.3$ for $U_{Mix} > 3.5\sqrt{gD}$, and Eq. (39) was used to calculate the void fraction.

Transition for declined flow at $-0.5°$ was observed to be due to the growth of long wavelength waves for $U_{SG} < 6$ m/s (Woods et al., 2000). This is confirmed by the agreement between predictions using VLW theory and the experimental data. The critical height in downflow is observed to be greater than the critical height in horizontal flows. This stabilizing effect of gravity is due to the reduction of the effects of liquid inertia, $\rho_L(C_R - \bar{u})^2$. For $U_{SG} > 6$ m/s, transition was observed to be due to the coalescence of K–H waves, as in horizontal flows. Measurements were not

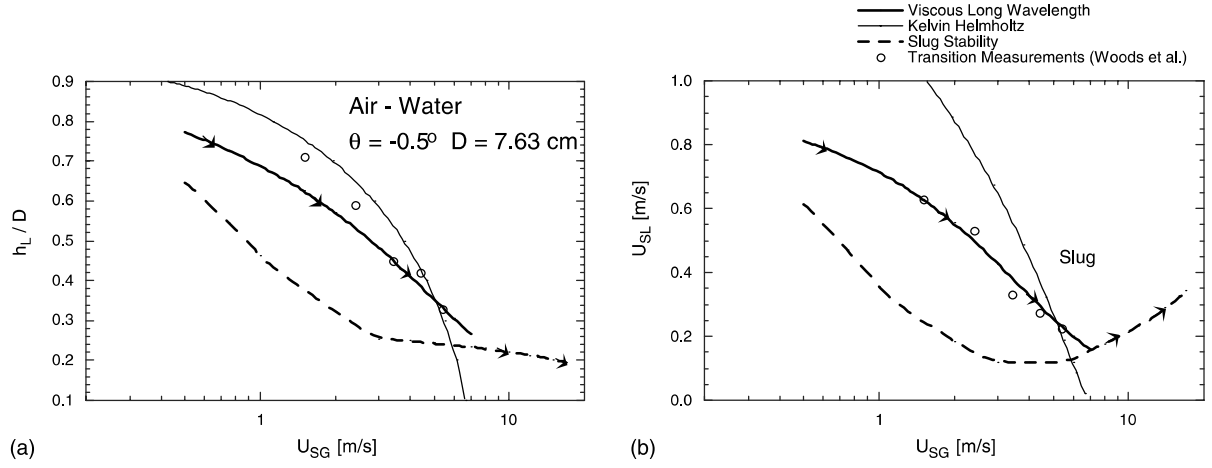

Fig. 9. Air–water theoretical predictions and downflow transition data, $D = 7.63$ cm.

reported at high velocities, but slug stability is believed to predict the transition boundary for $U_{SG} > 6$ m/s, as is suggested in Fig. 9.

Since the liquid interface is smooth at transition, the estimation of f_i/f_s should be good. As a consequence, the predictions of the critical U_{SL} are satisfactory.

5.6. Predictions for a natural gas pipeline

Calculations for flow of natural gas and natural gas condensate in a 20.3 cm pipe are given in Fig. 10. Kelvin–Helmholtz waves are predicted to occur at very low gas velocities in this system due to the high gas density and low surface tension. VLW waves should not play an important role in these flows, so predictions of their onset are not shown. The value of f_i/f_s was assumed to be given by Eq. (54) in the K–H predictions. In the slug stability calculations and the slug/plug boundary predictions, f_i/f_s was assumed to be given by Eq. (55). Hydraulic gradients were taken to be of the same order as was observed in the Freon gas–water flows ($dh/dx = -0.001$) for both slug stability and plug/slug boundary calculations. In the slug stability calculations, $s = 1$ for $U_{Mix} \leqslant 3.5\sqrt{gD}$ and $s = 1.3$ for $U_{Mix} > 3.5\sqrt{gD}$, and Eq. (39) was used to calculate the void fraction.

Measurements of the height of the liquid layer are not reported for the natural gas flows. Values of the critical height of the liquid layer obtained from K–H theory and from slug stability theory are shown. These calculations suggest that the coalescence of waves that have evolved from a K–H instability produces slugs. The critical conditions obtained from K–H theory are in a region where slugs are unstable. Therefore, transition is dictated by slug stability, in agreement with measurements of the critical U_{SL}. Plug flow is predicted to occur for $U_{SG} < 2$ m/s at $U_{SL} = 0.9$ m/s and at slightly lower U_{SG} as U_{SL} increases.

Critical h_L/D given by the Taitel–Dukler correlation are also shown in Fig. 10. These are quite different from what is predicted from slug stability, in that the TD critical U_{SL} are much smaller than the measurements.

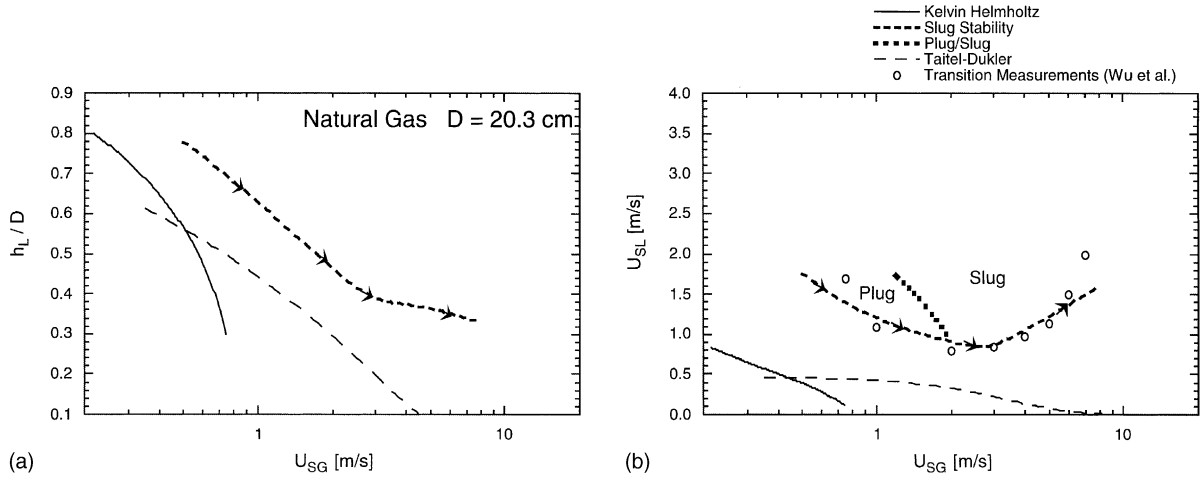

Fig. 10. Natural gas/condensate theoretical predictions and transition data, $D = 20.3$ cm.

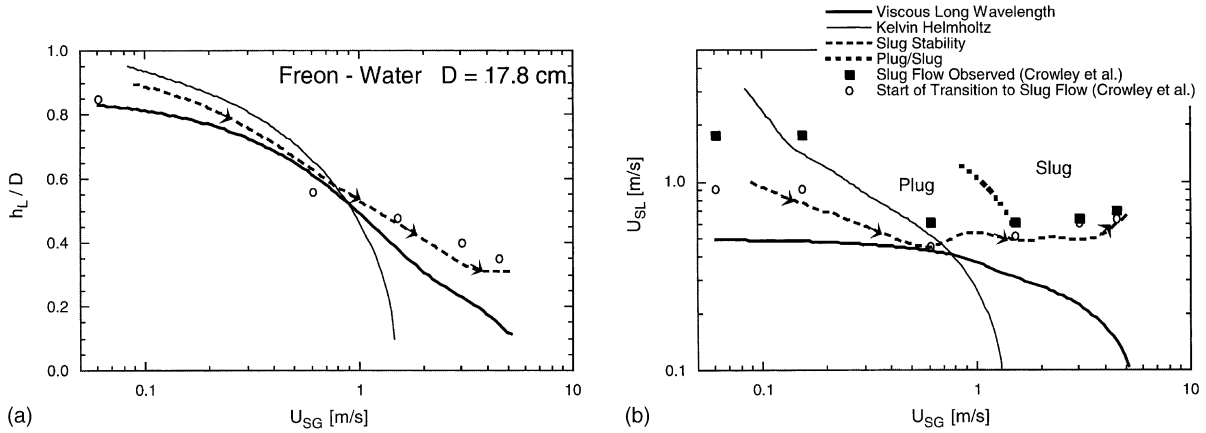

Fig. 11. Freon gas–water theoretical predictions and transition data, $D = 17.8$ cm.

5.7. Predictions for Freon gas–water

Fig. 11 compares theoretical predictions of the critical h_L/D and U_{SL} with measurements for the flow of Freon gas and water in a 17.8 cm pipe. In the calculations of the stability of a stratified flow to VLW waves, of slug stability, and of the plug/slug boundary, the friction factor ratio, f_i/f_s, was assumed to be given by Eqs. (54) and (55). Eq. (54) was used in predictions of the K–H instability. Hydraulic gradients were estimated using measured values reported by Crowley et al. (1986) $(dh/dx = -0.001)$ for $U_{SG} < 0.75$ m/s. In the slug stability calculations $s = 1$ for $U_{Mix} \leqslant 3.5\sqrt{gD}$ and $s = 1.3$ for $U_{Mix} > 3.5\sqrt{gD}$, and Eq. (39) was used to calculate the void fraction. At low gas velocities the critical h_L/D predicted by the VLW analysis are lower than what is predicted by K–H theory. However, this instability cannot lead to stable slugs or plugs at the predicted transition. Therefore, the criterion for slug or plug stability should define the critical conditions. At large gas velocities, irregular waves that evolve from a K–H instability should dominate the interface. Their coalescence leads to slugs if h_L/D is large enough for them to be stable.

A precise transition boundary is not given by Crowley et al. The transition zone is defined by the circles and squares in Fig. 11, with the boundary somewhere between these extremes. The measurements of the critical h_L/D and the critical U_{SL} agree with predictions from slug stability theory. Plug flow is predicted to occur for $U_{SG} < 1.5$ m/s at $U_{SL} = 0.55$ m/s and at slightly lower U_{SG} as U_{SL} increases.

6. Discussion

Theories used in this paper were developed in previous works. The contribution is the systematic comparison of available theories to experiments that cover a range of fluid properties and

pipe diameters. This allows the generality of the analyses to be judged. In the comparisons between predictions and experimental measurements, three different theories are found to define transition at low superficial gas velocities, that is VLW instability in air–water flows at low pressures, Kelvin–Helmholtz instability for viscous liquids, and slug stability in the two flows with high gas densities. At high gas velocities, transition is defined by slug stability theory in all cases considered.

The use of slug stability theory for the prediction of transition from stratified to intermittent flow differs from approaches that consider the stability of a stratified flow at low gas velocities and ad hoc assumptions about a critical h_L/D at large gas velocities, such as used by Taitel and Dukler (1976). In the case of high pressure natural gas/natural gas condensate flows this approach results in a significant improvement in the accuracy of predictions for all gas velocities, as seen in Fig. 10.

The accuracy of the theoretical calculations could be greatly improved if the interfacial friction factor, the liquid hydraulic gradients, the bubble velocity, the slug void fraction, and the slip ratio in the slug were better known over a wider range of fluid properties. The interfacial friction factor at transition is of critical importance since all of the theories are sensitive to the value of f_i/f_s that is used.

In slug stability theory, the relation between the bubble velocity and the mixture velocity is central to the accurate estimation of the critical height of the liquid layer. Improvement in the predictions could be realized if this dependence were measured more accurately at flow conditions near transition. Currently available measurements of bubble velocity were taken at large superficial liquid velocities, well above the transition values. The mixture velocity at which the laminar relation, Eq. (45), must be used to calculate the bubble velocity is not well established.

7. Flow regime prediction

It is appropriate to close this paper by outlining a methodology that can be used to predict the occurrence of slug and plug flows. The first step is to compare the heights of liquid layers needed for the onset of Kelvin–Helmholtz waves $(h_L/D)_{K-H}$, viscous long wavelength waves $(h_L/D)_{VLW}$, and for a slug to be stable $(h_L/D)_{SS}$. The onset of either K–H or VLW waves will define the transition if the liquid layer is high enough to sustain a stable slug. If h_L/D_{K-H} and $(h_L/D)_{VLW}$ are both greater than $(h_L/D)_{SS}$, then the lower of $(h_L/D)_{K-H}$ and $(h_L/D)_{VLW}$ is the height at which transition will occur. If $(h_L/D)_{SS}$ is greater than either $(h_L/D)_{K-H}$ or $(h_L/D)_{VLW}$, then $(h_L/D)_{SS}$ is the height at which transition will occur. This algorithm assumes that both K–H and VLW instabilities will occur. Once the transition height is known, the superficial liquid velocity at transition, U_{SL}, can be predicted from the liquid and gas momentum balance equations, Eqs. (6) and (7).

Acknowledgements

This work was supported by the Engineering Research Program of the Office of Basic Energy Sciences at the Department of Energy under DOE DEF G02-86ER 13556.

References

Andreussi, P., Bendiksen, K.H., 1989. Investigation of void fraction in liquid slugs for horizontal and inclined gas–liquid pipe flow. Int. J. Multiphase Flow 15, 937–946.

Andritsos, N., Hanratty, T.J., 1987a. Interfacial instabilities for horizontal gas–liquid flows in pipelines. Int. J. Multiphase Flow 13, 583–603.

Andritsos, N., Hanratty, T.J., 1987b. Influence of interfacial waves in stratified gas–liquid flows. AIChE J. 33, 444–454.

Andritsos, N., Williams, L., Hanratty, T.J., 1989. Effect of liquid viscosity on the stratified-slug transition in horizontal pipe flow. Int. J. Multiphase Flow 15, 877–892.

Bendiksen, K.H., 1984. An experimental investigation of the motion of long bubbles in inclined tubes. Int. J. Multiphase Flow 10, 467–483.

Bendiksen, K.H., Espedal, M., 1992. Onset of slugging in horizontal gas–liquid pipe flow. Int. J. Multiphase Flow 18, 234–247.

Benjamin, T.B., 1959. Shearing flow over a wavy boundary. J. Fluid Mech. 6, 161–205.

Benjamin, T.B., 1968. Gravity currents and related phenomena. J. Fluid Mech. 31, 209–248.

Bontozoglu, V., Hanratty, T.J., 1989. Wave height estimation in stratified gas–liquid flows. AIChE J. 35, 1346–1350.

Cohen, L.S., Hanratty, T.J., 1965. Generation of waves in the concurrent flow of air and a liquid. AIChE J. 11, 139–144.

Crowley, C.J., Sam, R.G., Rothe, P.H., 1986. Investigation of two-phase flow in horizontal and inclined pipes at large pipe size and high gas density. Report TN-399 for the Pipeline Research Committee, American Gas Association, Hanover, NH.

Dukler, A.E., Hubbard, M.G., 1985. A model for gas–liquid slug flow in horizontal tubes. Ind. Engng. Chem. Fund. 14, 337–347.

Fan, Z., Lusseyran, F., Hanratty, T.J., 1993. Initiation of slugs in horizontal gas–liquid flows. AIChE J. 39, 1741–1753.

Govier, G.W., Aziz, K., 1972. The Flow of Complex Mixtures in Pipes. Van Nostrand Reinhold Co., New York, p. 562.

Gregory, G.A., Scott, D.S., 1969. Correlation of liquid slug velocity and frequency in horizontal cocurrent gas–liquid slug flow. AIChE J. 15, 933–935.

Hanratty, T.J., Hershman, A., 1961. Initiation of roll waves. AIChE J. 7, 488–497.

Jeffreys, H., 1925. On the formation of water waves by wind. Proc. Roy. Soc. A 107, 189–206.

Kouba, G.E., Jepson, W.P., 1990. The flow of slugs in horizontal two-phase pipelins. Trans. ASME 112, 20–25.

Lighthill, M.J., Whitham, G.B., 1955. On kinematic waves. I. Flood movement in long rivers. II. Theory of traffic flow on long crowded roads. Proc. Roy. Soc. A 229, 281–345.

Lin, P.Y., Hanratty, T.J., 1986. Prediction of the initiation of slugs with linear stability theory. Int. J. Multiphase Flow 12, 79–98.

Lin, P.Y., Hanratty, T.J., 1987a. Detection of slug flow from pressure measurements. Int. J. Multiphase Flow 13, 13–21.

Lin, P.Y., Hanratty, T.J., 1987b. Effect of pipe diameter on flow patterns for air–water flow in horizontal pipes. Int. J. Multiphase Flow 13, 549–563.

Miles, J.W., 1957. On the generation of surface waves by shear flows. J. Fluid Mech 3, 185–204.

Milne-Thomson, L.M., 1968. Theoretical Hydrodynamics, fifth ed. The MacMillan Press, London.

Nydal, O.J., Pintus, S., Andreussi, P., 1992. Statistical characterization of slug flow in horizontal pipes. Int. J. Multiphase Flow 18, 439–453.

Ruder, Z., Hanratty, P.H., Hanratty, T.J., 1989. Necessary conditions for the existence of stable slugs. Int. J. Multiphase Flow 15, 209–226.

Ruder, Z., Hanratty, T.J., 1990. A definition of gas–liquid plus flow in horizontal pipes. Int. J. Multiphase Flow 16, 233–242.

Russell, T.W.F., Etchells, A.W., Jensen, R.H., Arruda, P.J., 1974. Pressure drop and holdup in stratified gas–liquid flow. AIChE J. 20, 664–669.

Sam, R.G., Crowley, C.J., 1986. Investigation of two-phase flow processes in coal slurry/hydrogen heaters. Creare Report TM-1085 for DOE.

Simmons, M.J.H., Hanratty, T.J., 2001. Transition from stratified to intermittent flow in small angle upflows. Int. J. Multiphase Flow 1, 509–516.

Taitel, Y., Dukler, A.E., 1976. A model for predicting flow regime transitions in horizontal and near horizontal gas–liquid flow. AIChE J 22, 47–55.

Wallis, G.B., Dobbins, J.E., 1973. The onset of slugging in horizontal stratified air–water flow. Int. J. Multiphase Flow 1, 325–335.

Woods, B.D., Hanratty, T.J., 1996. Relation of slug stability to shedding rate. Int. J. Multiphase Flow 22, 809–828.

Woods, B.D., Hurlburt, E.T., Hanratty, T.J., 2000. Mechanism of slug formation in downwardly inclined pipes. Int. J. Multiphase Flow 26, 977–998.

Woods, B.D., 1998. Slug formation and frequency of slugging in gas–liquid flows. Ph.D. Thesis, University of Illinois, Urbana.

Wu, H.L., Pots, B.F.M., Hollenburg, J.F., Mehoff, R., 1987. Flow pattern transitions in two-phase gas/condensate flow at high pressure in an 8-inch horizontal pipe. In: Proc. BHRA Conf., The Hague, The Netherlands, pp. 13–21.

Yih, C.S., 1969. Fluid Mechanics. McGraw-Hill, New York.